

Magnetoresistive effect in bulk composites 1-2-3 YBCO + CuO and 1-2-3 YBCO + BaPb_{1-x}Sn_xO₃ and their application as magnetic field sensors at 77 K

To cite this article: D A Balaev *et al* 2003 *Supercond. Sci. Technol.* **17** 175

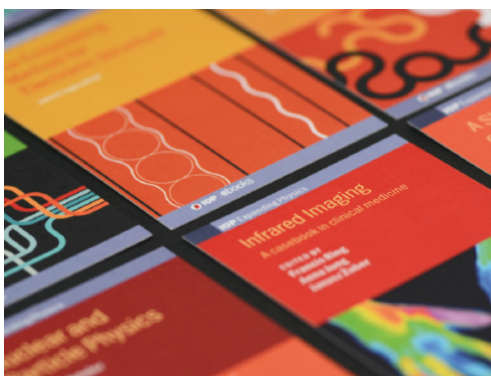
View the [article online](#) for updates and enhancements.

Related content

- [Study of dependence upon the magnetic field and transport current of the magnetoresistive effect in YBCO-based bulk composites](#)
D A Balaev, A G Prus, K A Shaykhutdinov *et al.*
- [Magnetoresistive effects in Bi-2212 melt textured bulk with MgO additions](#)
B Winton, M Ionescu, T Silver *et al.*
- [Thick films of superconducting YBCO as magnetic sensors](#)
B A Albiss

Recent citations

- [Study of Superconductivity in YBa₂Cu₃O_{7-x}/SrTiO₃ Composites](#)
T. Tchabukiani *et al*
- [Bi-based superconductors prepared with addition of CoFe₂O₄ for the design of a magnetic probe](#)
M.K. Ben Salem *et al*
- [Dominant influence of the compression effect of a magnetic flux in the intergranular medium of a granular high-temperature superconductor on dissipation processes in an external magnetic field](#)
D. A. Balaev *et al*



IOP | ebooks™

Bringing together innovative digital publishing with leading authors from the global scientific community.

Start exploring the collection—download the first chapter of every title for free.

Magnetoresistive effect in bulk composites 1-2-3 YBCO + CuO and 1-2-3 YBCO + BaPb_{1-x}Sn_xO₃ and their application as magnetic field sensors at 77 K

D A Balaev¹, K A Shaihtudinov¹, S I Popkov^{1,2}, D M Gokhfeld^{1,2}
and M I Petrov¹

¹ Kirensky Institute of Physics, 660036, Krasnoyarsk, Russia

² Reshetnev Siberian State Aerospace University, Krasnoyarsk 660014, Russia

E-mail: smp@iph.krasn.ru

Received 14 July 2003

Published 9 December 2003

Online at stacks.iop.org/SUST/17/175 (DOI: 10.1088/0953-2048/17/1/031)

Abstract

We have studied the magnetoresistive effect in bulk 1-2-3 YBCO + CuO and 1-2-3 YBCO + BaPb_{1-x}Sn_xO₃ composites prepared using the fast backing technique. We have found that the composites exhibit large magnetoresistance in low magnetic fields (<100 Oe) for a broad temperature range. We have studied the experimental dependences of resistivity versus magnetic field at various transport current densities. The high- T_C superconductor (HTSC) based composites exhibit a much higher sensitivity to weak magnetic fields at liquid nitrogen temperature, compared to that for pure HTSC ceramics. This effect is attractive for practical applications and the composite materials can be used as active elements in magnetic field sensor devices.

1. Introduction

The possible practical aspects of the application of bulk high- T_C superconductors (HTSCs) as magnetic field sensors were pointed out soon after the discovery of high-temperature superconductivity [1, 2]. Polycrystalline HTSCs exhibit large magnetoresistance in weak magnetic fields (tens of oersteds) [1–16]. This effect can be used in devices that demand a sensitive electrical response for a weak magnetic field. In this sense, polycrystalline bulk HTSCs are more attractive materials than conventional magnetic sensors which utilize the Hall effect or the magnetoresistive (MR) effect in semiconductors [1]. However, to the best of our knowledge, since 1988 up to the present date there have been no reports in the literature concerning devices in which bulk HTSCs would be magnetic field sensors. In our opinion, the following reasons discourage the practical application of bulk HTSCs as magnetic field sensors. (i) The temperature interval at which polycrystalline HTSCs exhibit a large magnetoresistance is very narrow, typically amounting to several degrees just below the critical temperature (85–90 K for the yttrium 1-2-3 HTSC

[3] and 90–100 K for the 2-2-2-3 bismuth HTSC [11]). The most convenient temperature at which the sensor would operate is the temperature of liquid nitrogen, but this is out of the range of the remarkable MR effect. (ii) There are small values of observed electrical response $R(H) - R(H=0)$, which is due to low resistivity of the HTSC in the normal state. (iii) In order to obtain a large enough response of magnetoresistance of bulk HTSC at 77 K, high transport current densities $j \sim 10^2 - 10^3 \text{ A cm}^{-2}$ [1, 2] or strong magnetic fields $H \sim 10 - 60 \text{ kOe}$ are required. In the former case, the Joule heat released at the HTSC/current lead contacts significantly distorts the voltage drop from the HTSC element. (iv) There is hysteretic behaviour of resistance R on the applied field [4, 6, 7, 9, 12, 13, 17]. (v) There is nonlinearity of the $R(H)$ dependence [1, 2, 4, 6–9, 12, 13, 17]. Moreover, the discovery of giant magnetoresistance in manganese oxides has significantly decreased the competitive ability of polycrystalline HTSCs as magnetic field sensors in comparison with these materials (see, for example, the review [18]).

Previously, we have studied the transport properties of bulk composites 1-2-3 YBCO + BaPb_{1-x}Sn_xO₃ [19, 20] and

1-2-3 YBCO + CuO [21, 22]. It has been shown that the composites represent a Josephson junction network, in which the non-superconducting component forms the barriers separating HTSC crystallites. The preliminary results of the effect of magnetic field on the $R(T)$ curves of composites are given in [23]. In this paper, we present the results of a detailed study of the MR effect in 1-2-3 YBCO + CuO and 1-2-3 YBCO + BaPb_{1-x}Sn_xO₃ composites. We show that most of the problems (i)–(v) listed above can be avoided by using these composites. Some parameters of the MR effect at weak magnetic fields obtained on the composites at 77 K at least are no worse than those of manganese oxides [18] in the sense of practical application.

2. Experimental details

2.1. Preparation and testing of the HTSC based composites

The preparation of the HTSC Y_{3/4}Lu_{1/4}Ba₂Cu₃O₇ is standard. CuO and metal-oxides BaPbO₃ and BaPb_{0.75}Sn_{0.25}O₃ are used as non-superconducting components of the composites.

Composite samples with 70–85 vol% of HTSC and 30–15 vol% CuO (high purity CuO powder is used) are prepared as follows. The components of the composite are thoroughly mixed, with additional common milling of the powders in the agate mortar, and then pressed into pellets. The pellets are placed in pre-heated boats and then placed in a furnace heated to a temperature of 910 °C. The pellets are kept at this temperature for 2 min and then placed in another furnace for 3 h at a temperature of 350 °C, which is followed by furnace cooling to room temperature.

BaPbO₃ and BaPb_{0.75}Sn_{0.25}O₃ are obtained from BaO₂, PbO and SnO₂ at 880 °C by the solid-state reaction technique. The x-ray diffraction (XRD) patterns of these compounds show only reflections from the perovskite structure. The values of resistivity at 77 K are 0.0057 Ω cm for BaPbO₃ and 0.0537 Ω cm for BaPb_{0.75}Sn_{0.25}O₃. Composite samples with 85 vol% of HTSC and 15 vol% BaPbO₃ or 15 vol% BaPb_{0.75}Sn_{0.25}O₃ have undergone a similar procedure as described above. The temperature regime is 5 min at 930 °C, then 6 h at 400 °C.

Hereafter we denote the composite samples as YBCO + VCuO, YBCO + VBaPbO₃, YBCO + VBaPb_{0.75}Sn_{0.25}O₃ where V is volume content of CuO, BaPbO₃ or BaPb_{0.75}Sn_{0.25}O₃ respectively, and the volume content of Y_{3/4}Lu_{1/4}Ba₂Cu₃O₇ is (100–V).

XRD patterns confirm the presence of both phases in the composites without any additional reflections. This fact indicates the absence of strong chemical interaction between the components of the composites. The average YBCO grain size is estimated to be 1.5 μm from the scanning electron microscopy (SEM) image. Magnetic measurements of the composites reveal a single superconducting phase in the samples with critical temperature $T_C = 93.5$ K similar to pure Y_{3/4}Lu_{1/4}Ba₂Cu₃O₇.

2.2. Electrical measurements

To measure the transport properties ($\rho(T)$ and $\rho(H)$ dependences and current–voltage (I – U) characteristics), the sample is cut from a sintered pellet in the form of parallelepiped

with typical dimensions $1 \times 1 \times 8$ mm³. The standard four-probe technique is used. The applied direct-current (dc) transport current density is varied in the range of ~ 0.004 – 1 A cm⁻². The accuracy of the indication of ‘zero resistance’ is $\sim 10^{-6}$ Ω cm. Copper solenoid is used for the generation of dc magnetic fields less than 500 Oe. Measurements in fields higher than 500 Oe have been performed using a superconducting solenoid ($H_{\max} = 60$ kOe). The transport current is perpendicular to the magnetic field direction. The samples have been cooled in zero magnetic field (the Earth magnetic field has not been screened). The I – U characteristics have been measured under constant dc conditions. The value of critical current density j_C is determined from the initial part of the I – U characteristics using the standard criterion $1 \mu\text{V cm}^{-1}$ [24].

3. Results and discussion

3.1. The effect of magnetic field on $R(T)$ dependences of the composites

Figures 1 and 2 show the temperature dependences of resistance of composites YBCO + CuO and YBCO + 15 BaPbO₃, YBCO + 15 BaPb_{0.75}Sn_{0.25}O₃ respectively, measured at different magnetic field strengths H (the values of transport current density j are shown). The sharp drop of resistance at 93.5 K observed in figures 1 and 2 is caused by the superconducting transition in HTSC crystallites. The critical temperature $T_C = 93.5$ K coincides with that observed for the Y_{3/4}Lu_{1/4}Ba₂Cu₃O₇ sample. A broad foot structure results from the transition of the network of weak links realized in the composites. Magnetic fields less than ~ 500 Oe affect mainly the second part of the resistive transition. The T_{C0} values decrease with the increase of H . The MR effect of the composites is observed for a broad temperature range in contrast to pure polycrystalline HTSCs [5, 8, 11]. Respectively, a weak magnetic field (~ 20 – 200 Oe) results in the growth of resistance of the composites from some value $\rho(H = 0)$ to the value $\rho(H)$. If $T < T_{C0}(H = 0)$, $\rho(H = 0) = 0$ (i.e., ρ is less than 10^{-6} Ω cm). The vertical dashed lines in figures 1 and 2, pictured as isotherms at 77 K, determine the possible magnitude of variation of resistance at this temperature caused by the magnetic field. The $\rho(T)$ curves measured at $H = 10$ and 60 kOe (figure 1(b)) exhibit smearing of the resistive transition in HTSC grains. The magnitude of this effect is comparable to that observed in single crystals [25]. We point out high values of $\rho(H)$ of the composites at weak magnetic field strengths with respect to that observed for pure polycrystalline YBa₂Cu₃O₇ ceramics [1, 2, 5–9, 17].

The physical mechanism of the MR effect of polycrystalline HTSC has been discussed in the literature (see, for example, [1, 3, 5, 6, 8–16]) and can briefly be considered as follows. It is well known that the resistive state of granular HTSCs is governed by intergrain boundaries which are weak links of Josephson type. Respectively, a small magnetic field suppresses the critical current of a Josephson junction and results in the appearance of a junction resistance [24]. Each grain boundary in percolation traces of transport current flowing through polycrystalline HTSCs contributes to the electrical response of the whole sample. This is the

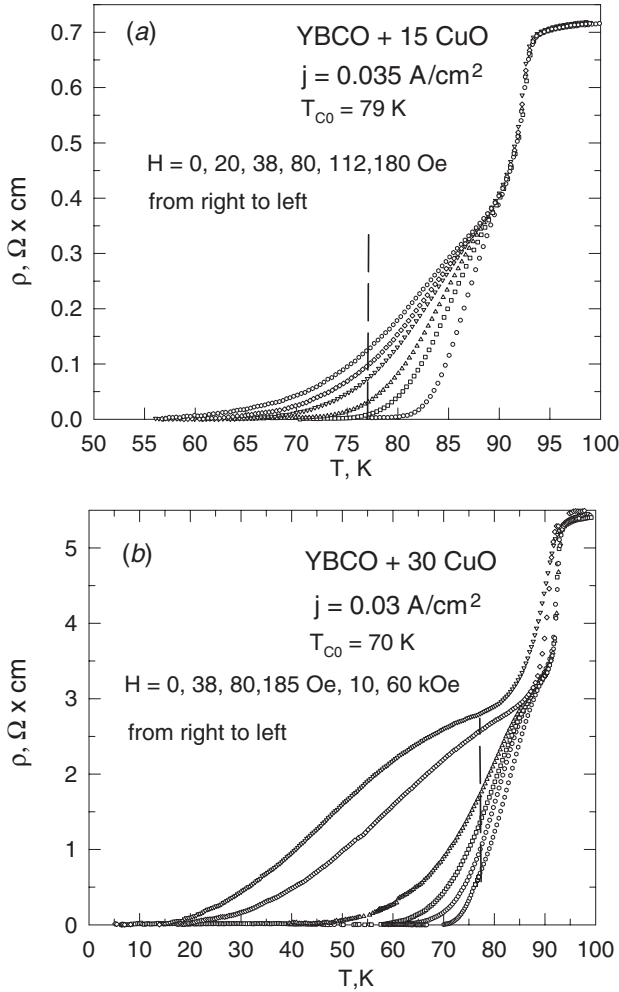


Figure 1. Experimental dependences of the resistivity of composites YBCO + 15 CuO (a) and YBCO + 30 CuO (b) measured at various magnetic field strengths H . The H values are given in the figures. The vertical dashed lines (isotherms at 77 K) indicate the possible response of the resistance of the weak-link network caused by the magnetic field.

physical background of the MR effect in granular HTSCs. A detailed comparison of experimental data $R(T, H)$ obtained on ceramic HTSCs with theoretical models of the MR effect in a Josephson junction network has been carried out in the literature; see, for example, [14–16, 25].

Figure 3 shows the experimental dependences of resistive transition width $\Delta T_{C0} = T_{C0}(H = 0) - T_{C0}(H)$ versus $H^{2/3}$ for the studied composites in the range $0 < H \lesssim 300 \text{ Oe}$. The experimental points fit well to the straight lines with the slopes $C \approx 0.7 \text{ K Oe}^{-2/3}$ for YBCO + 15 CuO, $\approx 0.85 \text{ K Oe}^{-2/3}$ for YBCO + 30 CuO, $\approx 1 \text{ K Oe}^{-2/3}$ for YBCO + 15 BaPbO₃, and $\approx 1.25 \text{ K Oe}^{-2/3}$ for YBCO + 15 BaPb_{0.75}Sn_{0.25}O₃. The behaviour observed is explained in the framework of the Tinkham theory of resistive transition in HTSCs [25]. The dependence $\Delta T_{C0} = CH^{2/3}$ was observed on pure HTSC ceramics in the low field range [5, 25]. The typical value of the factor C is $\approx 0.155 \text{ K Oe}^{-2/3}$ for polycrystalline YBa₂Cu₃O₇ [5]. So, the mechanism of resistive transition under the influence of the magnetic field is concluded to be similar both for the composites under study and for polycrystalline HTSCs,

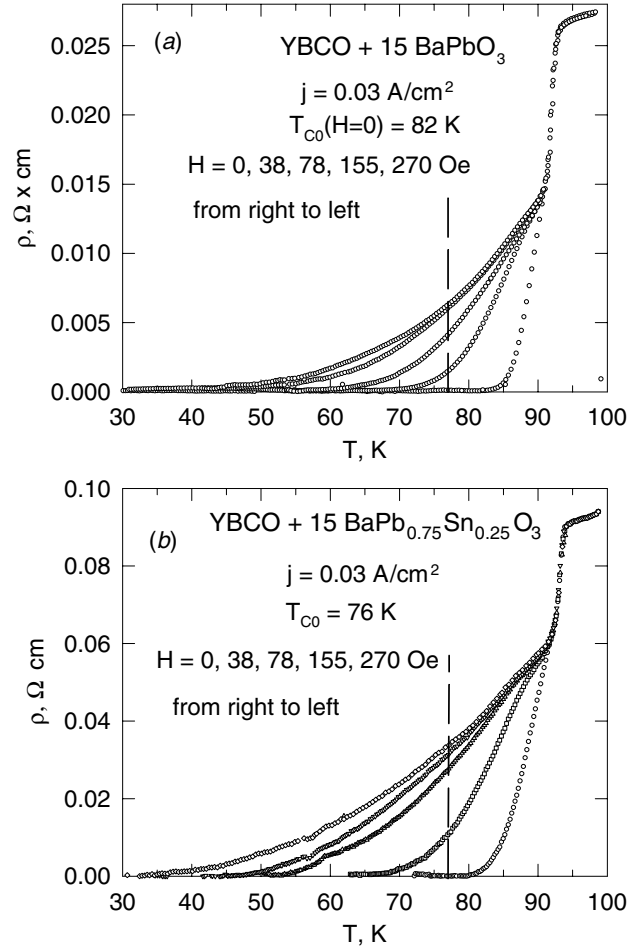


Figure 2. Experimental dependences of the resistivity of composites YBCO + 15 BaPbO₃ (a) and YBCO + 15 BaPb_{0.75}Sn_{0.25}O₃ (b) measured at various magnetic field strengths H . The H values are given in the figures. The vertical dashed lines (isotherms at 77 K) indicate the possible response of the resistance of the weak-link network caused by the magnetic field.

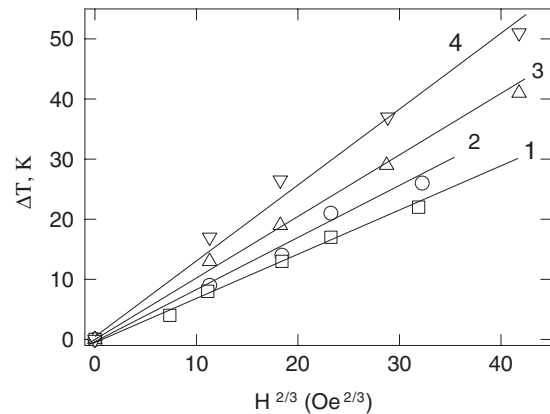


Figure 3. Experimental dependences of $\Delta T_{C0} = T_{C0}(H = 0) - T_{C0}(H)$ versus $H^{2/3}$ for the composites: 1, YBCO + 15 CuO; 2, YBCO + 30 CuO; 3, YBCO + 15 BaPbO₃; 4, YBCO + 15 BaPb_{0.75}Sn_{0.25}O₃.

while the factor C is significantly higher in the former case. According to [25], the parameter C is inversely proportional to the critical current density $j_C(0 \text{ K})$. The non-superconducting

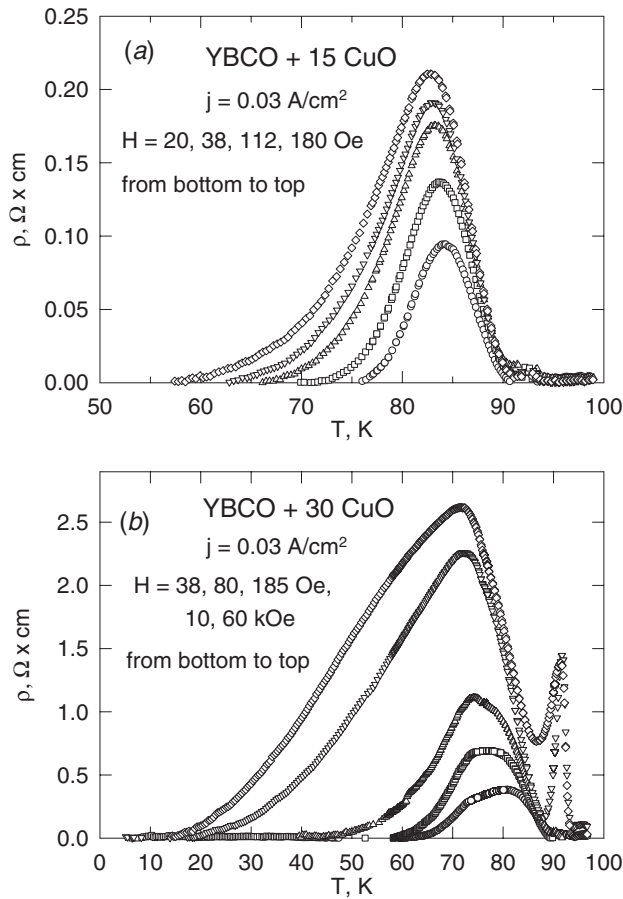


Figure 4. Excess resistivity $\Delta\rho(T, H) = \rho(T, H) - \rho(T, H = 0)$ (from figure 1) for samples YBCO + 15 CuO (a) and YBCO + 30 CuO (b) for various magnetic fields.

ingredient of a composite is a material forming Josephson weak links between the HTSC crystallites. This results in suppression of Josephson coupling (lower values of j_C and T_{C0} than for pure polycrystalline HTSCs) and, as a consequence, in a wide temperature range of the MR effect of the composites.

3.2. Excess resistance caused by magnetic field

Figure 4 shows the temperature dependences of excess resistivity $\Delta\rho(T, H) = \rho(T, H) - \rho(T, H = 0)$ (i.e., the difference between $\rho(T, H)$ and $\rho(T, H = 0)$ from figure 1) of composites YBCO + CuO caused by the magnetic field. The dependences $\Delta\rho(T, H)$ are characterized by the bell-shaped curve with maximum shifting to low temperatures with an increase of magnetic field. Similar behaviour of $\Delta\rho(T, H)$ is observed for YBCO + 15 BaPbO₃ and YBCO + 15 BaPb_{0.75}Sn_{0.25}O₃ samples (not shown). We processed experimental $\rho(T, H)$ curves obtained on pure polycrystalline YBa₂Cu₃O₇ [5] ceramic in order to derive $\Delta\rho(T, H)$ dependences. These dependences were found to have a similar bell-shaped form as the composites but the temperature interval of the ‘bell’ was about $\sim 2 \text{ K}$ at $H \approx 50 \text{ Oe}$ ($T_C \approx 91.5 \text{ K}$). The strong dependence of excess resistance of bulk HTSCs on temperature at fixed H implies that, for the magnetic field sensor to work correctly, the temperature

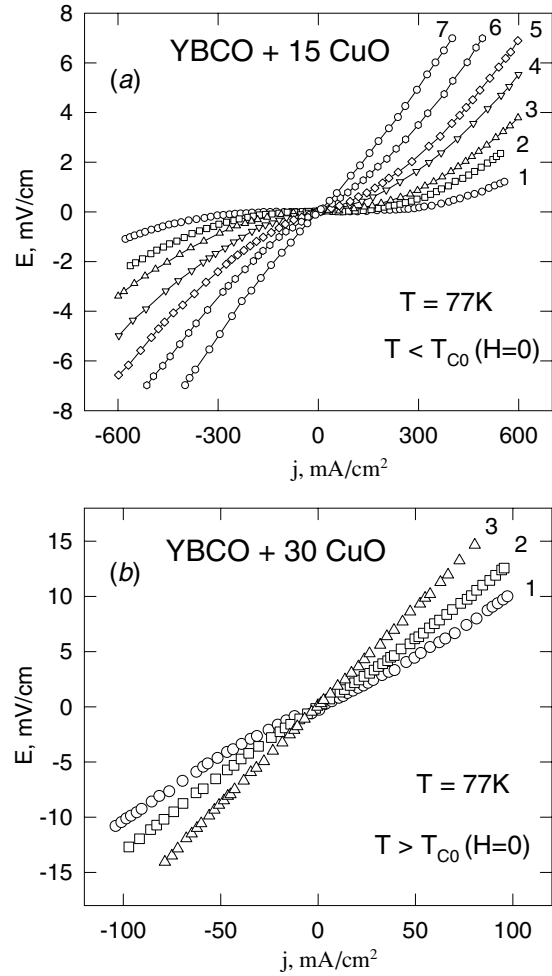


Figure 5. Initial parts of the $I-U$ characteristics of composites YBCO + 15 CuO (a) and YBCO + 30 CuO (b) at 77 K measured at various magnetic field strengths: (a) $H = 0$ (curve 1), 4 Oe (curve 2), 15 Oe (curve 3), 27 Oe (curve 4), 38 Oe (curve 5), 64 Oe (curve 6), 207 Oe (curve 7); (b) $H = 0$ (curve 1), 23 Oe (curve 2), 207 Oe (curve 3).

of the HTSC element must be held with very high accuracy. Figure 4 clearly shows the effect of an increase in CuO content in composites YBCO + CuO on the position of maximums of $\Delta\rho(T, H)$. The maximum of $\Delta\rho(T)$ at $H = 185 \text{ Oe}$ of sample YBCO + 30 CuO is close to 77 K. By varying the volume content of the non-superconducting ingredient (CuO or BaPbO₃, etc) in the composite we can shift the temperature of maximal excess resistivity to any required value in the range below T_C including $T = 77 \text{ K}$.

3.3. Resistance–magnetic field dependences

3.3.1. The effect of magnetic field on $I-U$ characteristics.

The magnitude of MR effect in composites depends on transport current because the $I-U$ curves of the composites are nonlinear in the whole temperature range below T_C . At $T < T_{C0}$ the $I-U$ curves are characterized by the existence of the critical current. A typical $I-U$ curve with a portion of $U < 10^{-6} \text{ V cm}^{-1}$ is presented in figure 5(a), with the sample YBCO + 15 CuO. T_{C0} is $\approx 79 \text{ K}$ at $H = 0$ for this sample. For the composite YBCO + 30 CuO, $T_{C0} \approx 70 \text{ K}$ at $H = 0$.

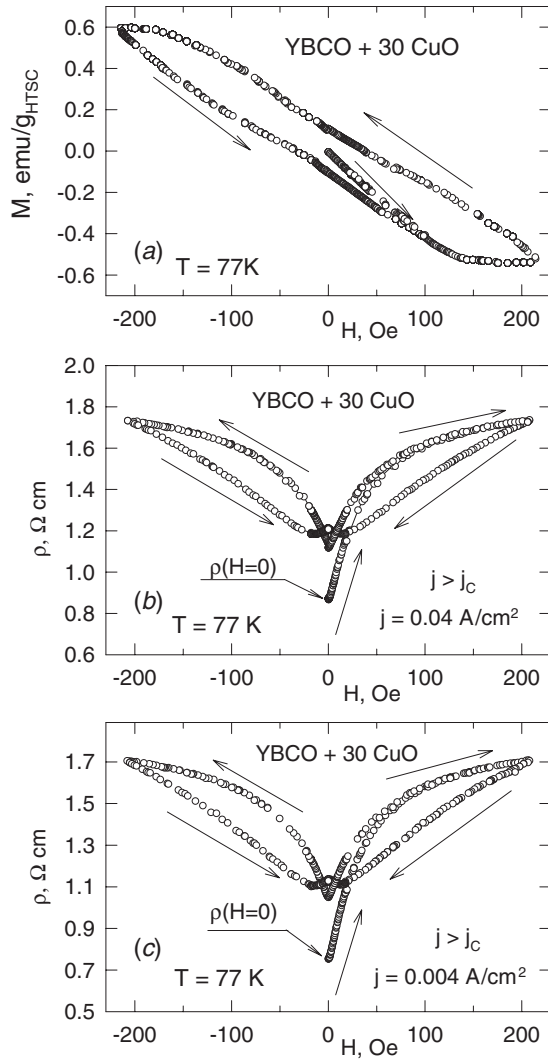


Figure 6. Experimental magnetic field dependences of magnetization measured by a vibrating sample magnetometer (a) and resistivity (b), (c) of sample YBCO + 30 CuO at 77 K. The values of scanning current are given in the figures. Arrows indicate the direction of scanning of the magnetic field. The value of $\rho(H=0)$ is determined in (b) and (c). Case 3 ($j > j_c$) takes place for both $\rho(H)$ curves (b), (c).

Figure 5(b) shows the $I-U$ dependence of this sample at 77 K. The $I-U$ curve grows from the point of origin and is strongly nonlinear. The influence of the magnetic field on the initial part of the $I-U$ characteristics is seen from figures 5(a) and (b).

3.3.2. Hysteretic behaviour of the $\rho(H)$ dependences. The magnetic field dependences of the resistance $\rho(H)$ of composites have been measured at different temperatures. Below, we present the $\rho(H)$ data at 77 K because these are of practical interest.

Figures 6(b) and (c) and figures 7(b) and (c) show experimental $\rho(H)$ curves of composites YBCO + 30 CuO and YBCO + 15 BaPbO₃ respectively, measured at various transport current densities. The modification of the $\rho(H)$ loops with the increase of transport current is seen from figures 6 and 7. At $T = 77$ K in the magnetic field range–

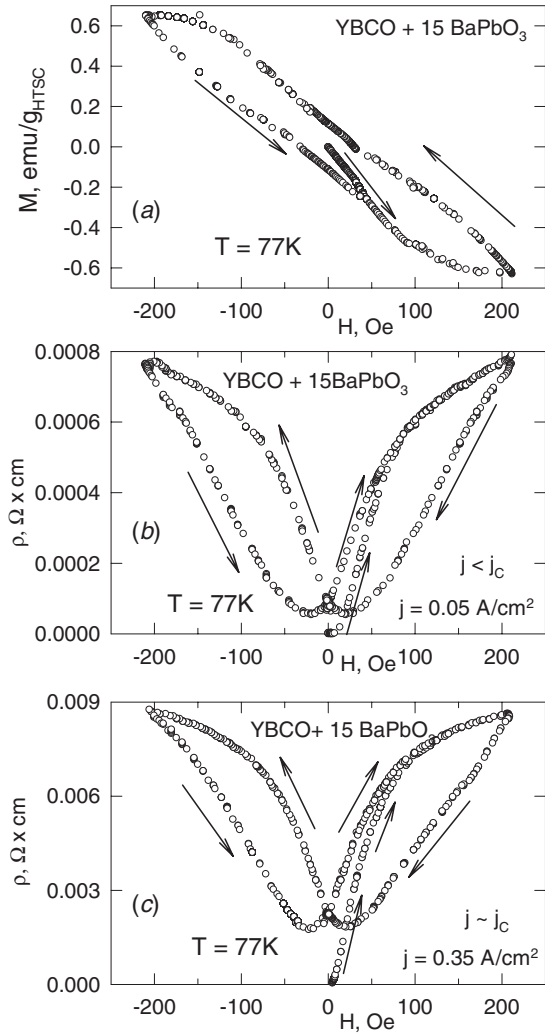


Figure 7. Experimental magnetic field dependences of magnetization measured by a vibrating sample magnetometer (a) and resistivity (b), (c) of sample YBCO + 15 BaPbO₃ at 77 K. The values of scanning current are given in the figures. Arrows indicate the direction of scanning of the magnetic field. Case 1 ($j < j_c$) takes place for (b), and case 2 ($j \approx j_c$) takes place for (c).

$37 \lesssim H \lesssim 37$ Oe the $\rho(H)$ curves are reversible. When the magnetic field is increased further, the $\rho(H)$ dependences demonstrate hysteresis, which results in residual resistance after the decrease of the field to zero. Such behaviour was observed earlier on HTSCs [6, 7, 12, 13, 17, 26]. The hysteresis of the $\rho(H)$ dependence is connected with the magnetization hysteresis loop $M(H)$ [3, 6, 9, 10, 12, 13]. The $M(H)$ curves of composites YBCO + 30 CuO and YBCO + 15 BaPbO₃ presented in figures 6(a) and 7(a) have been measured on the same specimens and in the same magnetic field ranges ($-210 \leq H \leq 210$ Oe) as the corresponding $\rho(H)$ dependences. The irreversibility field from $M(H)$ curves coincides with that obtained from $\rho(H)$ measurements ($H_{irr} \approx 37$ Oe). The dependence of resistance on the magnetization of samples is seen to be very complicated as resistance R is a function of transport current. Processing of experimental $R(H, j)$ curves in terms of models for percolating HTSCs [12, 13, 16, 25] as well as the derivation of $R(M)$ dependence will be carried out in the future.

3.3.3. *Initial branch of $\rho(H)$ curves.* Now, we focus on the initial branch of the $\rho(H)$ dependence of the composites. The character of the $\rho(H)$ curves is found to depend on the relationship between bias current j and critical current j_C . If current j is less than its critical value, $j/j_C < 1$ (case 1), there is a part of $\rho(H)$ where $\rho \leq 10^{-6} \Omega \text{ cm}$. Starting from some threshold field H_C , nonlinear $\rho(H)$ dependence takes place. Figure 7(b) shows this behaviour for composite YBCO + 15 BaPbO₃ ($H_C \approx 9 \text{ Oe}$). For composite YBCO + 15 CuO, $H_C \approx 10 \text{ Oe}$ at $j = 0.03 \text{ A cm}^{-2}$ and $T = 77 \text{ K}$ (not shown). The magnitude of H_C is easily varied by the value of the transport current. The $\rho(H)$ curve measured at current $j \approx j_C$, $j/j_C \approx 1$ (case 2) grows from the point of origin. Figure 7(c) shows the $\rho(H)$ dependence typical for case 2. Further increasing the transport current, $j/j_C > 1$ (case 3), transforms the initial part of the $\rho(H)$ curve, which starts to grow from some non-zero value $\rho(H = 0)$. Figures 6(b) and (c) show the $\rho(H)$ dependences of composite YBCO + 30 CuO at 77 K. When $T_{C0} < 77 \text{ K}$ for this sample (see figure 1(b)), the value $j_C(77 \text{ K})$ is negligibly small (less than $10^{-5} \text{ A cm}^{-2}$). For this reason, the condition of case 3 takes place at any transport current. A similar picture is observed for composite YBCO + 15 BaPb_{0.75}Sn_{0.25}O₃ because its T_{C0} value is $\approx 76 \text{ K}$. The largest response of resistance takes place for case 3. It is seen from a comparison of the data from figures 6(b), 6(c), 7(c) and figures 1 and 2 that more than 50% of the possible increase of resistance occurs in fields less than 100 Oe.

Under the condition of case 3, the $\rho(H)$ dependences of composites with insulator (CuO) and metal-oxide (BaPb_{1-x}Sn_xO₃) demonstrate different behaviours. The $\rho(H)$ dependences of YBCO + 15 BaPb_{1-x}Sn_xO₃ composites are nonlinear in the whole field range. On the other hand, the initial part of the $\rho(H)$ dependence of the YBCO + CuO composites is linear. The range where $\rho(H)$ dependences obey the law $\rho(H) = \rho(H = 0) + (d\rho/dH) \times H$ comes to $0 \leq H \lesssim 20 \text{ Oe}$ for the YBCO + 15 CuO sample and $0 \leq H \lesssim 12 \text{ Oe}$ for YBCO + 30 CuO (these $\rho(H)$ dependences are presented in figure 8 on an enlarged scale). The values $d\rho/dH$ in these ranges are $2.5 \text{ m}\Omega \text{ cm Oe}^{-1}$ for the YBCO + 15 CuO sample and $17.5 \text{ m}\Omega \text{ cm Oe}^{-1}$ for the YBCO + 30 CuO sample. The parameter $d\rho/dH$ is the sensitivity of resistivity of a material to the magnetic field. The values of $d\rho/dH$ obtained on YBCO + CuO composites are two to three orders of magnitude more than those estimated by us from the $\rho(H)$ curves of 'pure' YBa₂Cu₃O₇ ceramics in [1, 2] at 77 K ($d\rho/dH \approx 0.15 \text{ m}\Omega \text{ cm Oe}^{-1}$ [1] and $d\rho/dH \approx 0.005 \text{ m}\Omega \text{ cm Oe}^{-1}$ [2]).

The high values of $\Delta\rho(H) = \rho(H) - \rho(H = 0)$ and $d\rho/dH$ for the YBCO + CuO composites, as compared to those for pure HTSC ceramics, can be explained as follows. It was shown in [21, 22] that, in the YBCO + CuO composites prepared by the fast baking technique, the transport current flows through both HTSC and CuO grains. The resistivity of CuO is very high at low temperatures ($> 10^{12} \Omega \text{ cm}$ below 100 K [27]). This results in an exponential growth of resistivity of the composites in the normal state with an increase of CuO content [22]. The use of an insulator (which does not interact with the HTSC) as the non-superconducting component of the composite allows us to obtain the sensitive electrical response of a composite to the weak magnetic field.

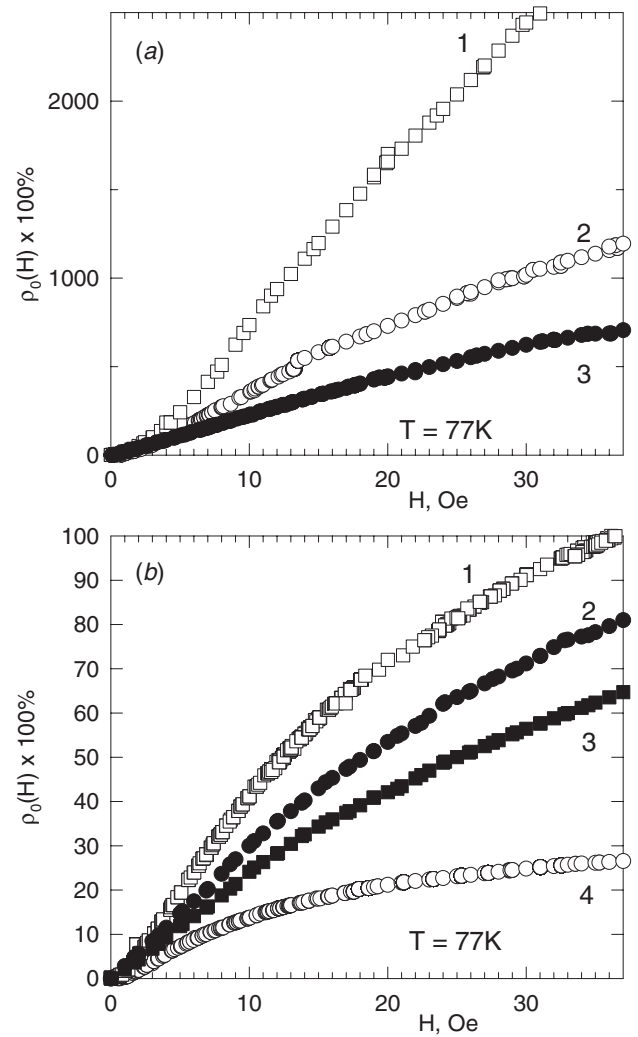


Figure 8. The dependences $\rho_0(H) \times 100\%$ ($\rho_0(H) = [\rho(H) - \rho(H = 0)]/\rho(H = 0)$) of YBCO + CuO (closed symbols) and YBCO + BaPbO₃ (open symbols) composites at 77 K in the reversible H range. (a) 1, YBCO + 15BaPbO₃, $j = 0.7 \text{ A cm}^{-2}$, $\rho(H = 0) = 0.19 \text{ m}\Omega \text{ cm}$; 2, YBCO + 15BaPb_{0.75}Sn_{0.25}O₃, $j = 0.037 \text{ A cm}^{-2}$, $\rho(H = 0) = 1.9 \text{ m}\Omega \text{ cm}$; 3, YBCO + 15 CuO, $j = 0.4 \text{ A cm}^{-2}$, $\rho(H = 0) = 12 \text{ m}\Omega \text{ cm}$. (b) 1, YBCO + 15 BaPb_{0.75}Sn_{0.25}O₃, $j = 0.37 \text{ A cm}^{-2}$, $\rho(H = 0) = 0.02 \Omega \text{ cm}$; 2, YBCO + 30 CuO, $j = 0.004 \text{ A cm}^{-2}$, $\rho(H = 0) = 0.725 \Omega \text{ cm}$; 3, YBCO + 30 CuO, $j = 0.04 \text{ A cm}^{-2}$, $\rho(H = 0) = 0.83 \Omega \text{ cm}$; 4, YBCO + 15 BaPb_{0.75}Sn_{0.25}O₃, $j = 0.925 \text{ A cm}^{-2}$, $\rho(H = 0) = 0.042 \Omega \text{ cm}$.

3.3.4. *The $\rho_0(H)$ dependences.* The value $\rho_0 = [\rho(H = 0) - \rho(H)]/\rho(H = 0)$ is an important parameter for sensor devices especially for digital operations [1, 18]. This parameter characterizes the relative variation (increase or decrease) of the resistivity of a material under the influence of an external magnetic field. It is clear that for case 1, where $\rho(H = 0)$ is typically less than $10^{-6} \Omega \text{ cm}$, the value ρ_0 reaches enormous magnitude. However, the more suitable condition for practical applications would be the variation of resistivity in relation to a not extremely small value $\rho(H = 0)$. This circumstance takes place for case 3 described above. Figure 8 shows the $\rho_0(H)$ dependences for the composites in the reversible magnetic field range. The magnitude of ρ_0 may reach thousands of per cent

while $\rho(H = 0)$ values are not too small (0.2–10 m Ω cm; see the caption to figure 8). The linear part of the $\rho(H)$ dependences for YBCO + CuO composites is clearly seen from figures 8(a) and (b).

4. Concluding remarks

The composites YBCO + CuO and YBCO + BaPbO₃ prepared by the fast baking technique exhibit large enough MR effect in a wide temperature range including the liquid nitrogen temperature, which is convenient for practical applications. The composites possess a high sensitivity of resistivity to a weak magnetic field (<200 Oe) $\Delta\rho(H) = \rho(H) - \rho(H = 0)$, compared to that for pure polycrystalline HTSCs. There is a linear part on the resistance–magnetic field dependence obtained on the YBCO + CuO composites under the condition $j > j_C$ in the range $0 \leq H \lesssim 20$ Oe. The $\rho(H)$ dependences are reversible in the range $|H| \lesssim 37$ Oe at 77 K. The magnitudes of transport current density j used in this work are small enough (~ 1 A cm⁻²) and do not result in the heating of samples during measurements, in contrast to pure HTSC ceramics whose j_C values are of the order of 10–100 A cm⁻² [1, 2, 7–9, 19] at 77 K. The reported facts point to the possible use of HTSC based composite materials as bulk magnetic field sensors operating at 77 K in a wide range of applications in electronic devices.

We can list the following types of possible application of HTSC based composites as active elements of magnetic field sensors.

Type 1. The detection of a magnetic field in the range $0 \lesssim H \lesssim 20$ Oe using the linear part of $\rho(H)$ dependence.

Type 2. The technique of multiply increasing the resistance with respect to some value $\rho(H = 0)$ for digital operations in microelectronic devices. Large values of $\rho_0 = (\rho(H) - \rho(H = 0))/\rho(H = 0)$ (up to thousands of per cent) may be achieved on the composites with respect to $\rho(H = 0) \sim 0.2$ –10 m Ω cm at 77 K.

Type 3. The response of sensor resistance at some threshold magnetic field value H_C (case 1, see section 3.3.3). The H_C value can be easily ruled by the magnitude of transport current and volume content of the non-superconducting ingredient, but it would be less than the irreversibility field ($H_{irr} \approx 37$ Oe at 77 K for our samples).

5. Conclusion

We believe that the experimental results reported in this paper can allow us to take a fresh look at bulk HTSC based materials as magnetic field sensors. The composites possess high sensitivity of resistivity for magnetic fields compared to that of pure polycrystalline HTSCs. In the range of weak magnetic fields, i.e., tens of Oe, where the MR effect is reversible ($H_{irr} \approx 37$ Oe at 77 K), the values of parameter ρ_0 obtained on the composites do not yield to those of manganese oxides. The sign of the reported MR effect is positive in contrast to

that for manganese oxides. This may be important for some devices.

Acknowledgments

This work was partially supported by a joint programme of RFBR and KRSF ‘Enisey’, grant 02-02-97711, and by the Siberian Branch of the Russian Academy of Sciences in the framework of the Lavrent’ev competition of Young Scientists Projects of 2002.

References

- [1] Nojima H, Tsuchimoto S and Kataoka S 1988 *Japan. J. Appl. Phys.* **27** 746
- [2] Ohnuma T, Kuroko T and Ishii M 1989 *Proc. ISEC 1989 (Tokyo)* p 206
- [3] Mitin A V 1994 *Sverkhprovodn., Fiz. Khim. Tekh.* **7** 62
- [4] Kojevnikov V L, Krylov K P, Ponomarev A I, Sadovskii M V, Tsidil’kovskii I M and Cheshnitskii S M 1987 *Fiz. Met. Metalloved.* **64** 184
- [5] Dubson M A, Herbert S T, Calabrese J J, Harris D C, Patton B R and Garland J C 1988 *Phys. Rev. Lett.* **60** 1061
- [6] Shifang S, Yong Z, Guoqiang P, Daoqi Yu, Han Z, Zuyao C, Yitai Q, Weiyang K and Qirui Z 1988 *Europhys. Lett.* **6** 359
- [7] Kopelevich Ya V, Lemanov V V, Sonin E B and Syrnikov P P 1988 *Fiz. Tverd. Tela* **30** 2432
- [8] Aronzon B A, Gershanov Yu V, Meilikhov E Z and Shapiro V G 1989 *Sverkhprovodn., Fiz. Khim. Tekh.* **2** 83
- [9] Kopelevich Ya V, Lemanov V V and Makarov V V 1991 *Fiz. Tverd. Tela* **32** 2313
- [10] Mitin A V 1994 *Physica C* **235–240** 3311
- [11] Wright A C, Zhang K and Erbil A 1991 *Phys. Rev. B* **44** 863
- [12] Kuz’michev N D 2001 *Pis’ma Zh. Eksp. Teor. Fiz.* **74** 291
- [13] Kuz’michev N D 2001 *Fiz. Tverd. Tela* **43** 1934
- [14] Shakeripour H and Akhavan M 2001 *Supercond. Sci. Technol.* **14** 234
- [15] Mohammadzadeh M R and Akhavan M 2003 *Supercond. Sci. Technol.* **16** 538
- [16] Burlachkov L, Mogilko E, Schlesinger Y and Havlin S 2003 *Phys. Rev. B* **67** 104509
- [17] Qian Y J, Tang Z M, Chen K Y, Zhou B, Qui J W, Miao B C and Cai Y M 1989 *Phys. Rev. B* **39** 4701
- [18] Nagaev E L 1996 *Usp. Fiz. Nauk* **166** 833
- [19] Petrov M I, Balaev D A, Ospishchev S V, Shaihtudinov K A, Khrustalev B P and Aleksandrov K S 1997 *Phys. Lett. A* **237** 85
- [20] Petrov M I, Balaev D A, Gokhfeld D M, Ospishchev S V, Shaihtudinov K A and Aleksandrov K S 1999 *Physica C* **314** 362
- [21] Petrov M I, Balaev D A, Shaihtudinov K A and Aleksandrov K S 1999 *Phys. Solid State* **41** 881
- [22] Petrov M I, Balaev D A, Shaihtudinov K A and Aleksandrov K S 2001 *Supercond. Sci. Technol.* **14** 798
- [23] Balaev D A, Gokhfeld D M, Popkov S I, Shaihtudinov K A and Petrov M I 2001 *Tech. Phys. Lett.* **27** 952
- [24] Barone A and Paterno J 1982 *Physics and Application of the Josephson Effect* (New York: Wiley)
- [25] Tinkham M 1988 *Phys. Rev. Lett.* **61** 1658
- [26] Afanas’ev N V, Vasyutin M A, Golovashkin A I, Grigorashvili Yu V, Ivanova L I, Kuz’michev N D, Motulevich G P and Rusakov A P 1989 *Pis’ma Zh. Eksp. Teor. Fiz.* **15** 55
- [27] Gizhevskii B A, Samokhvalov A A, Chebotaev N M, Naumov S V and Pokazan’eva G K 1991 *Sverkhprovodn., Fiz. Khim. Tekh.* **4** 827